ISSN 2277-3061

Ant-Snake model for Linear Feature Extraction from Satellite Image

Jalal Amini
Department of Surveying Engineering, Faculty of Engineering, University of Tehran, Tehran, Iran
E-mail: jamini@ut.ac.ir
Leila Mohammadnia
Pakdasht Kharazmi Research, Pakdasht, Iran.
E-mail: lmohamadnia@gmail.com

ABSTRACT

This paper proposes an optimized mathematical model for linear feature extraction from satellite images. The model is based on a developed ant colony model combined with the snake model (called Ant-Snake model) to identify and extract the linear features like roads from satellite images. The process is started with the developed ant colony model to recognize and identify interest object and then with a snake model extract object. The developed ant model is able to establish a pheromone matrix that represents the object information at each pixel position of the image, according to the movements of a number of ants which are dispatch to move on the image. And the snake model is a parametric curve which is allowed to deform from some arbitrary initial locations from pheromone matrix toward the desired final location by minimizing an energy function. Experimental results are provided to demonstrate the superior performance of the proposed approach.

Keywords

Ant colony; Linear feature; Road extraction; **S**atellite image**;** Snake.

1. Introduction

Automatic objects extraction from remotely sensed images requires the formulation of procedures and knowledge that indicate the content of the images. The structure of these objects in images is complex. Specially, when the resolution is increased, the content in the objects becomes considerably more complex.

Extraction of linear objects like road from **s**atellite images is also one of the main problems in the automatic mapping. In literature, there are many papers published to automatic and semi-automatic linear feature extraction. Gruen and Li developed a linear feature extraction method using snakes[1]. They combined the characteristics of snakes and adaptive least squares correlation method.

Barzohar and Cooper proposed an automatic method of extracting main roads in aerial images[2]. The aerial image is partitioned into windows, road extraction start from the window of high confidence estimates, while road tracing is to perform a dynamic programming to find an optimal global estimate. Park and Kim presented a road extraction algorithm using template matching[3].

Tupin et al. studied the automatic extraction of the road network in dense urban areas using a few metres resolution SAR images based on different orientation views [4]and Markov random. Katartzis et al described a model-based method for the automatic extraction of linear features from aerial images[5]. Byoung et al. developed a technique to extract roads in a space-borne SAR image using a genetic algorithm[6]. Amini et al., applied the fuzzy sets for roads identification from high-resolution images[7]- [8]. Bentabet et al. presented an approach for roads detection from SAR images and road databases, and the approach included developing a restoration filter and a line plausibility calculation step[9]. Wessel and Wiedemann studied automatic road extraction from airborne SAR imagery[10]. Long and Zhao proposed a new integrated system for automatic extraction of main linear feature in high-resolution optical satellite images[11]. Zhu et al. also proposed a new developed approach to extract road network from high resolution satellite images[12]. The approach is based on the binary and grayscale mathematical morphology and a line segment match method. Yang and Wang presented an improved model for road detection based on the principals of perceptual organization and classification fusion in human vision system[13]. Based on this literature, when we use automatic methods for linear feature extraction, it is necessary to make identify roads from images. In this paper an approach is presented to extract the features like roads in vector form from the satellite images.

In summary, the objectives of this paper are:

1- Proposed a model based on the developed ant colony and minimizing the snake energy for identifying and extraction linear feature.

2- Showed the capability of our proposed algorithm on satellite images in detection and extraction roads.

The first stage is identifying and detecting roads with the developed ant colony model from the pre-processed satellite image. The skeleton of the identified roads is extracted using mathematical morphology operators in the second stage and then the road centerline vectors are extracted using a snake interpolated model.

The rest of this paper is organized as follows: Section 2 discusses the developed ant colony model for identifying the roads. Section 3 explains the mathematical morphology and snakes for road vector extraction and the experimental results will be discussed in section 4 and finally, section 5 presents the concluding remarks.

2- The Developed Ant Colony in Identifying the Linear feature

The aim of Ant Colony (AC) is iteratively find the optimal solution of the problem through a guided search over the solution space, by constructing the *pheromone* information. Suppose totally K ants are applied to find the optimal solution in a space χ that consists of M1 × M2 nodes. There are two fundamental issues in the AC process; that is, the establishment of the probabilistic transition matrix $p^{(n)}$ and the update of the pheromone matrix $\tau^{(n)}$.

First, at the *n*-th construction-step of AC, the *k*-th ant moves from the node *i* to the node *j* according to a probabilistic action rule, which is determined by [14]

$$p_{i,j}^{n} = \frac{\left(\tau_{i,j}^{(n-1)}\right)^{\alpha}\left(\eta_{i,j}\right)^{\beta}}{\sum_{j \in \sum \Omega_i}\left(\tau_{i,j}^{(n-1)}\right)^{\alpha}\left(\eta_{i,j}\right)^{\beta}} \quad if \;\; j \in \Omega_i \qquad (1)$$

Where $\tau_{i,j}^{n-1}$ is the pheromone information value of the arc linking the node *i* to the node *j*; Ω_i is the neighborhood nodes for the ant a_k given that it is on the node *i*; the constants α and β represent the influence of pheromone information and heuristic information, respectively; $\eta_{i,j}$ represents the heuristic information for going from node *i* to node *j*, which is fixed to be same for each construction-step.

Second, the pheromone matrix needs to be updated twice during the AC procedure. The first update is performed after the movement of *each* ant within each construction step. After the move of the *k*-th ant within the *n*-th construction-step, the pheromone matrix is updated as [14]

$$\tau_{i,j}^{n-1} = \begin{cases} (1-\rho)\ \tau_{i,j}^{(n-1)} + \rho\,\Delta_{i,j}^{(k)} & if\,(i,j)\ belongs\,to\ the\ tour \\ \tau_{i,j}^{(n-1)} & 0 \qquad therwise \end{cases} \qquad (2)$$

Where ρ is the *evaporation rate*. Furthermore, the determination of *best tour* is subject to the user-defined criterion, it could be either the best tour found in the current construction-step, or the best solution found since the start of the algorithm, or a combination of both of the above two. The second update is performed after the move of all *K* ants within each construction-step; and the pheromone matrix is updated as[14]:

$$\tau^{(n)} = (1-\psi)\ \tau^{(n-1)} + \psi\ \tau^{(0)} \qquad (3)$$

Where ψ is the *pheromone decay coefficient*. Note that the ant colony system performs two update operations (i.e, (2) and (3)) for updating the pheromone matrix) [15].

The developed AC is based on to utilize a number of ants to move on a 2-D image for constructing a pheromone matrix and then identifying the roads regions. The movements of the ants are steered by the local variation of the image's intensity values[16].

The proposed approach starts from the *initialization process* by ants. Then the ants start for moving on the image to find the interest regions related to roads based on the road characteristics. From the new locations of each ant, the process runs for N iterations to construct the pheromone matrix by iteratively performing both the *construction process* and the *update process*. Finally, the *decision process* is performed to determine and identify the roads.

For the *identification process* in detail, assume totally K ants are assigned on the roads of image **I** with a size of M1 ×M2, each pixel of which can be viewed as a node. The initial value of each component of the pheromone matrix $\tau^{(0)}$ is set to be a constant. τ_{init}

At the *n*-th construction step, one ant is randomly selected from the above-mentioned total K ants, and this ant will consecutively move on the image for L movement steps. This ant moves from the node (*l*,*m*) to its neighboring node (*i, j*) according to a transition probability that is defined as

$$p_{(l,m),(i,j)}^{n} = \frac{\left(\tau_{i,j}^{(n-1)}\right)^{\alpha}\left(\eta_{i,j}\right)^{\beta}}{\sum_{(i,j)\in\sum\Omega_{(l,m)}}\left(\tau_{i,j}^{(n-1)}\right)^{\alpha}\left(\eta_{i,j}\right)^{\beta}} \qquad (4)$$

where $\tau_{i,j}^{n-1}$ is the pheromone value of the node (*i*, *j*), $\Omega_{(l,m)}$ is the neighborhood nodes of the node (*l*,*m*), $\eta_{i,j}$ represents the heuristic information at the node (*i*, *j*).

There are two crucial issues in the construction process. The first issue is the determination of the heuristic information $\eta_{i,j}$ in (4). In this paper, it is proposed to be determined by the local statistics at the pixel position (*i, j*) as

$$\eta_{i,j} = (I(i,j) - I_m(i,j))^2 \qquad (5)$$

where $I(i,j)$ is the intensity value of the pixel at the position (*i*, *j*) of the image **I**. $I_m(i,j)$ is mean value of the intensity values of a window with size of 3×3 centered on (*i*,*j*). $\eta_{i,j}$ value depends on the variation of image's intensity values on the window.

The second issue is to determine the permissible range of the ant's movement in (4)) at the position (*l*,*m*). In this paper, it is proposed to be either the 4-connectivity neighborhood or the 8-connectivity neighborhood, both of which are demonstrated in Figure 1.

ISSN 2277-3061

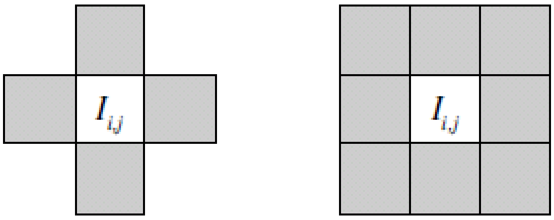

(a) **(b)**

Figure1.the ants movement in (a) 4-connectiving and (b) 8-connectiving

The proposed approach performs two updates operations for updating the pheromone matrix.

- The first update is performed after the movement of each ant within each construction-step. Each component of the pheromone matrix is updated according to

$$\tau_{i,j}^{n-1} = \begin{cases} (1-\rho)\,\tau_{i,j}^{(n-1)} + \rho\,\Delta_{i,j}^{(k)} & if\,(i,j)\ \ is\ visited\ by the current\ k-th\ ant \\ \tau_{i,j}^{(n-1)} & otherwise \end{cases} \qquad (6)$$

where ρ is defined in (2), $\Delta_{i,j}^{(k)}$ is determined by the heuristic matrix; that is, $\Delta_{i,j}^{(k)} = \eta_{i,j}$

- The second update is carried out after the movement of all ants within each construction-step according to

$$\tau^{(n)} = (1-\psi)\,\tau^{(n-1)} + \psi\,\tau^{(0)} \quad (7)$$

where ψ is defined in (3).

In. *decision process* a binary decision is made at each pixel location to determine whether it is edge or not, by applying threshold T on the final pheromone matrix $T^{(N)}$. In this paper, the above-mentioned T is proposed to be adaptively computed based on the method developed in [20].

The initial threshold $T^{(0)}$ is selected as the mean value of the pheromone matrix. Next, the entries of the pheromone matrix is classified into two categories according to the criterion that its value is lower than $T^{(0)}$ or larger than $T^{(0)}$. Then the new threshold is computed as the average of two mean values of each of above two categories. The above process is repeated until the threshold value does not change any more (in terms of a user-defined tolerance). The above iterative procedure can be summarized as follows.

Step 1: Initialize $T^{(0)}$ as:

$$T^{(0)} = \frac{\sum_{i=1:M_1} \sum_{j=1:M_2} \tau_{i,j}^{(N)}}{M_1 \; M_2} \qquad (8)$$

And set the iteration index as l = 0.

Step 2: Separate the pheromone matrix $T^{(N)}$ into two class using $T^{(l)}$, where the fist class consists entries of **τ** that have smaller values than $T^{(l)}$, while the second class consists the rest entries of **τ.** Next, calculate the mean of each of the above two categories via

$$m_L^{(l)} = \frac{\sum_{i=1:M_1} \sum_{j=1:M_2} g_{T^{(l)}}^{L} \quad (\tau_{i,j}^{(N)})}{\sum_{i=1:M_1} \sum_{j=1:M\,2} h_{T^{(l)}}^{L} \; (\tau_{i,j}^{(N)})} \qquad (9)$$

ISSN 2277-3061

$$m_U^{(l)} = \frac{\sum_{i=1:M_1} \sum_{j=1:M_2} g_{T(}^{U} \quad (\tau_{i,j}^{(N)})}{\sum_{i=1:M_1} \sum_{j=1:M2} h_{T^{(l)}}^{U} \quad (\tau_{i,j}^{(N)})} \qquad (10)$$

$$g_{T^{(l)}}^{L} = \begin{cases} x & if \;\; x \le T^{(l)} \\ 0 & otherwise \end{cases} \qquad (11)$$

$$h_{T^{(l)}}^{L} = \begin{cases} 1 & if \;\; x \le T^{(l)} \\ 0 & otherwise \end{cases} \qquad (12)$$

$$g_{T^{(l)}}^{U} = \begin{cases} x & if \;\; x \ge T^{(l)} \\ 0 & otherwise \end{cases} \qquad (13)$$

$$h_{T^{(l)}}^{U} = \begin{cases} 1 & if \;\; x \ge T^{(l)} \\ 0 & otherwise \end{cases} \qquad (14)$$

Step 3: Set the iteration index l = l + 1, and update the threshold as

$$T^{(L)} = \frac{m_L^{(l)} + m_U^{(l)}}{2} \qquad (15)$$

Step 4: If $\left|T^{(l)} - T^{(n-1)}\right| \succ \varepsilon$, then go to *Step 2*; otherwise, the iteration process is terminated and a binary decision is made on each pixel position (i, j) to determine whether it is edge (i.e., $E_{i,j} = 1$) or not (i.e. $E_{i,j} = 1$)

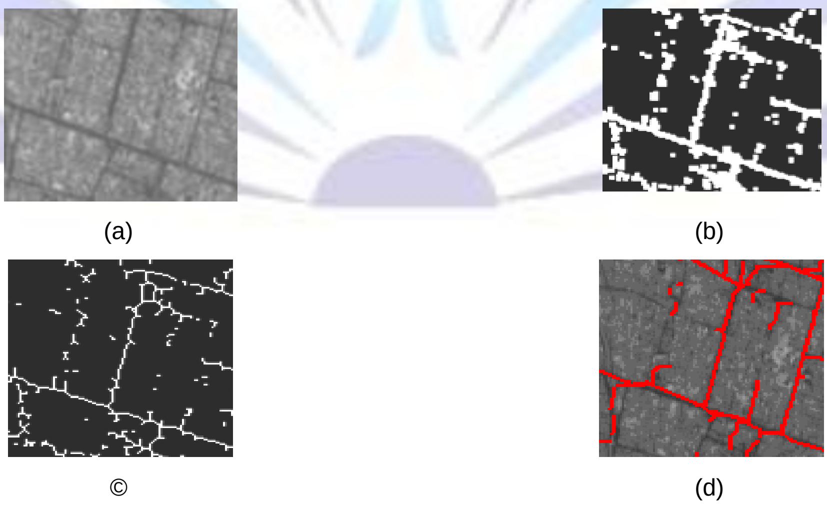

Figure 2(a) original image (b) identified road, (c) smoothed skeleton, (d) extracted road vector

3-Road Vectors Extraction

Extraction of road vectors centerline is the last stage in the block diagram of figure1. Thus, the mathematical morphology is first used for extraction of skeletons from the identified roads image in the previous section and then used a snake model for extraction of roads in the geometric form.

Mathematical morphology is a powerful tool in image processing for extraction of skeleton. The basic operations in mathematical morphology are erosion, dilation, opening, and closing.

The skeleton of the identified roads in the binary image is extracted by thinning algorithm that works iteratively in the mathematical morphology. In each iteration, pixels from the boundary of objects are removed using structure element until the final thinned image consists only lines with one pixel width and isolated points. Here, the structure element $L^{(4)}$ is defined as follows**[7]**:

$$L_1^{(4)} = \begin{bmatrix} 0\,0\,0 \\ *\,1\,* \\ 1\,1\,1 \end{bmatrix}; \quad L_2^{(4)} = \begin{bmatrix} *\,0\,* \\ 1\,1\,0 \\ 1\,1\,* \end{bmatrix} \qquad (8)$$

Because usually there are some legs and isolated short lines on the outline of the objects, it is possible to remove legs and smooth the main skeleton sequentially by another structure element, $E^{(4)}$**, [7]**. The structure element $E^{(4)}$ is defined as follows:

$$E_1^{(4)} = \begin{bmatrix} *\,*\,* \\ 0\,1\,0 \\ *\,0\,* \end{bmatrix}; \quad E_2^{(4)} = \begin{bmatrix} *\,0\,* \\ 0\,1\,* \\ *\,0\,* \end{bmatrix} \qquad (9)$$

'*' in the matrixes denotes an element that is not used in the matching process, i.e. its value is not significant. Figure 3 shows the processing result by the morphology operators on the identified road image (figure 3(b) and Figure 3(c) shows the smoothed skeleton. Finally, a snake model is applied on figure 3(c) to extract the roads in vector form.

A snake is a parametric curve which is allowed to deform from some arbitrary initial location toward the desired final location by minimizing an energy function. In the continues domain, the snake is defined as a parametric curve, *r*(*s*,*t*) =(*x*(*s*,*t*), *y*(*s*,*t*)), where *s* is a parameter advancing along the snake and *t* is related to arc length. The snake minimizes an energy function based on internal and external constraints at time *t.*

$$E_{tot}(r(s,t)) = \eta E_{\text{int}}(r(s,t)) + E_{ext}(r(s,t)) \qquad (10)$$

Where: E_{ext} is the external energy, E_{int} is the internal energy and η is a regularization parameter. The energy function is built such that its global minimum coincides with the solution r_0

$$r_0 = \min_r E_{tot}(r(s,t)) \qquad (11)$$

Based on Bentabet et al. [9], the problem is to determine the curve r_0 such as

$$r_0 = \min_r \left[\int_S \alpha \left\| \frac{\partial r(s,t)}{\partial s} \right\|^2 + \beta \left\| \frac{\partial^2 r(s,t)}{ds^2} \right\|^2 .ds - \int_S \lambda(r(s,t))ds \right] \qquad (12)$$

The equation (8) dose not admits any analytical solution. Using Euler-Lagrange equation ($\nabla E_{tot} = 0$), it can be proved that the local minimum of energy must satisfy

$$-\alpha \frac{\partial^2 r(s,t)}{ds^2} + \beta \frac{\partial^4 r(s,t)}{ds^4} = -\frac{\partial \lambda(r(s,t))}{\partial r} \qquad (13)$$

It is assumed that α and β remain constant along the snake. The derivative term $\frac{\partial}{\partial r}$ in the right-hand side of the equation (13) is a vector derivative which can be decomposed in terms of $\partial/\partial x$ and $\partial/\partial y$. It requires the computation of the curve forth-order derivative which might cause numerical stability problems. A lagrangian evolution is obtained by introducing a first-order derivative term which is considered as an internal term

$$\gamma \frac{\partial r(s,t)}{\partial t} - \alpha \frac{\partial^2 r(s,t)}{ds^2} + \beta \frac{\partial^4 r(s,t)}{ds^4} = -\frac{\partial \lambda(r(s,t))}{\partial r} \qquad (14)$$

ISSN 2277-3061

Where: *r* represents the viscosity of the background. The partial derivative equations are usually implemented using finite elements[17] -[18]. This method offers an accurate discritization of the derivative, leading to greater accuracy. Discretizing the parametric curve *r*(*s*,*t*), for $t = t_0$, into finite elements leads an expression for each elements, given by

$$r^e(s) = \langle \mathbf{N}(s) \rangle . [\mathbf{V}^e]$$

Where: <…> denotes row vectors and […] matrices or column vectors. N(s) is a set of shape or basis functions $\langle \mathbf{N}_1(s), \mathbf{N}_2(s), ..., \mathbf{N}_m(s) \rangle$ defining the interpolating curves and $[\mathbf{V}^e]$ is a two column matrix, $[\mathbf{X}^e, \mathbf{Y}^e]$, of control points. Thus, as shown in figure 8, the curve (here road) *r*(*s*) can be approximated using finite elements $r^e(s)$

$$r(s) = \sum_{e=1}^{N} r^e(s) \qquad (15)$$

Therefore, the minimization of E_{tot}^e for each element leads to $\partial E_{tot}^e / \partial V^e = 0$, thus

$$(\alpha.[k_1] + \beta[k_2]).[\mathbf{V}^e] + [f^e] = [k^e].[\mathbf{V}^e] + [f^e] = 0 \qquad (16)$$

Where: $[K_1] = \int_S [\mathbf{N}_s].\langle \mathbf{N}_s \rangle ds$; $[K_2] = \int_S [\mathbf{N}_{ss}].\langle \mathbf{N}_{ss} \rangle ds$

$[f^e]$ is the external forces vector applied on the control nodes of element *e* of the snake.

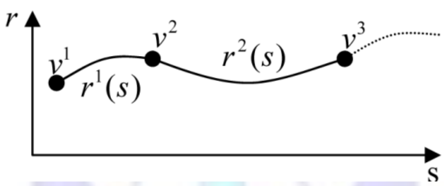

Figure 3. elements of a road

The above process is applied on figure 2(c) to extract the road vectors form. Figure 2(d) shows the extracted roads in vector forms that can be used in a data base layer for many applications.

4. Experimental Results

The proposed model applied to a number of satellite images. In this section, an example with results will be given. The original image contain main roads with wide of 2 –3 pixels. Figure 4(a) shows the original image and the extracted roads that are laid over the original image is shown in figure 4(e). Main roads have been identified and only a few roads have not been detected. This is due to width of some roads is less than 2 pixel . And some pixels are also detected incorrectly so that they correspond to other classes such as agricultural lands.

For geometric accuracy assessment of the algorithm, two types of roads in the original images are considered: main roads with width of 2 to 3 pixels or more and other roads with width of 1 to 2 pixels, these roads are extracted both manually as reference and automatically so that the accuracy of results could be assessed. Two measures: mean of residuals and root mean square error (RMSE) are obtained by calculating the actual distance between extracted road points and reference roads. Table 1 shows the results of the geometric accuracy assessment.

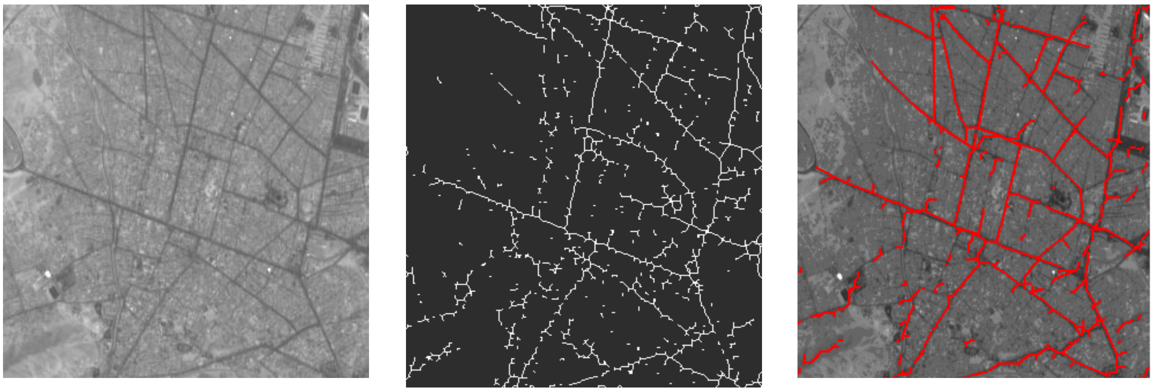

(a) (b) (c)

Figure 4 (a) original image (b) extracted skeleton (c) extracted roads

Table 1. Accuracy of the algorithm for automatic roads extraction.

Type of road	*Width of road (Pixel)*	*Mean error (Pixel)*	*RMS Error(Pixel)*
Main roads	2-3	1.5	0.61
Other roads	*1-2*	*1.6*	*0.63*

5. Conclusions

This paper developed a method (called Ant-Snake) for identifying and extracting linear feature such as roads from satellite images. The method was based on the improved ant colony model combined with the snake model to identifying and extracting the linear feature from satellite images.

The proposed approach indicated that is efficient in road vectors extraction from this type of images using the ant colony and the snake model for identification of roads centerlines and extraction of roads in vector form were the main aim of this paper. The accuracy of extracted road vectors was evaluated both visually and quantitatively. From point of view in visually, the extracted roads was very close to the roads on the original image. From point of view in quantitatively, the statistical results confirmed that the proposed approach is also efficient, so that the achieved accuracy was approximately 0.60 pixel for examples in this study.

6. References

[1] GRUEN, A. and LI, H., (1997), Semiautomatic linear feature extraction by dynamic programming and LSB_Snakes. Photogrammetric Engineering & Remote Sensing, 63, pp. 985-995.

[2] BARZOHAR, M .D. B. COOPER, (1996), Automatic finding of main roads in aerial images by using

Geometric Stochastic models and estimation, IEEE trans. PAMI, Vol.18, No.7, pp. 707-721

[3] PARK S. R.,T. KIM, (2001), Semi-Automatic road extraction algorithm from IKONOS images using

template matching, Proc. 22nd Asian Conference on remote Sensing, pp. 1209-1213.

[4] TUPIN, F., HOUSHMAND, B. and DATCU, M., (2002), Road detection in dense urban areas using SAR imagery and the usefulness of multiple views. IEEE Transactions on Geoscience and Remote Sensing, 40, pp. 2405–2414.

[5] KATARTZIS, A., PIZURICA, V. and SAHLI, H., (2001), Application of mathematical morphology and Markov Random Field theory to the automatic extraction of linear features in airborne images. In Mathematical Morphology and its Applications to Image Processing, J. Goutsias, L. Vincent and D.S. Bloomberg (Eds) (Boston/Dordrecht/ London: Kluwer Academic), pp. 405–414.

[6] BYOUNG, K.J., JANG, J.H. and HONG, K.S., (2002), Road detection in spaceborne SAR images using a genetic algorithm. IEEE Transactions on Geoscience and Remote Sensing, 40, pp. 22–29.

[7] AMINI, J. SARADJIAN M.R., BLAIS, J.A.R., LUCAS, C., and AZIZI, A., (2002(a)), Automatic road-side extraction from large scale imagemaps, International journal of Applied Earth Observation and Geoinforamtion, 4, pp. 95-107.

[8] AMINI, J., LUCAS C., SARADJIAN M.R., AZIZI A., and SADEGHIAN S., (2002(b)), Fuzzy logic system for road identification using Ikonos images, The Photogrammetric record, Vol. 17 (99), pp.493-503.

[9] BENTABET, L., JODOUIN, S., ZIOU, D. and VAILLANCOURT, J., (2003), Road vectors update using SAR imagery: a snake-based method. IEEE Transactions on Geoscience and Remote Sensing, 41, pp. 1785–1803.

[10] WESSEL, B. and WIEDEMANN, C., (2003), Analysis of automatic road extraction results from

airborne SAR imagery. ISPRS Archives, XXXIV, Part 3/W8.

[11] LONG, H., and ZHAO, Z., (2005), Urban road extraction from high-resolution optical satellite images, International journal of remote sensing, Vol. 26, No. 22, pp: 4907-4921.

[12] Zhu, C., Wang, Y., Ma, Q. and Shi, W. (2004). 'Road extraction from high-resolution remotely sensed image based on morphological segmentation', Acta Geodaetica et Cartographics Sinica, (33) 4.

[13] YANG, J. AND WANG R. S., (2007), Classified road detection from satellite images based on perceptual organization, International journal of remote sensing, Vol. 28, No. 20, pp: 4653-4669.

[14] M. Dorigo, M. Birattari, and T. Stutzle, "Ant colony optimization," IEEE Computational Intelligence Magazine, vol. 1, pp. 28–39, Nov. 2006.

[15] M. Dorigo and L. M. Gambardella, "Ant colony system: A cooperative elearning approach to the traveling salesman problem," IEEE Trans. On Evolutionary Computation, vol. 1, pp. 53–66, Apr. 1997

[16] Jing Tian, Weiyu Yu, and Shengli Xie. An Ant Colony Optimization Algorithm For Image Edge Detection, Vis. Applicat., 2008.

[17] COHEN, L. D., and COHEN, I, (1993), Finite element methods for active contour models and balloons for 2-D and 3-D images, IEEE Transactions on Pattern Anal. and Machine Intell. Vol. 15, pp. 1131–1147

[18] LIANG, J., MCLNERNY, T., and TERZOPOULOS, D., (1999), United snakes, in IEEE 7th int. Conf. Computer Vision, pp: 933-940.

Author's Biography with Photo

Jalal Amini was born in Mashhad, Iran, in 1969. He received the B.Sc. degree in surveying engineering from the K.N.Tossi University, Tehran, Iran, in 1993, the M.S. degree in photogrammetry from the K.N.Tossi University, Tehran, Iran, in 1996, and the Ph.D degree in photogrammetry and remote sensing from university of Tehran, Tehran, Iran, in 2001. He is currently as associate professor of remote sensing with the department of geomatics engineering, University of Tehran, Tehran, Iran. His experience includes automatic object extraction (roads) from satellite images, Mathematic modelling of space images, morphology, neural networks, fuzzy sets, fractals, DEM, classification, alpha-shapes, floodplain delineation, and microwave remote sensing including SAR signal processing.

Leila Mohamadnia was born in kashmar, Iran, in 1978. she received the M.S. degree in applied mathematics ,numerical analysis from the Iran University of Science and Technology in 2007. She received the Ph. D . degree in applied mathematics ,numerical analysis from the Department of mathematic, Science and Research Branch, Islamic Azad University, Tehran, Iran in 2012. Her experience includes automatic object extraction (roads) from satellite images, Mathematic modelling of space images.